LIDOCAINE BLOCKAGE OF BASOLATERAL POTASSIUM CHANNELS IN THE AMPHIBIAN URINARY BLADDER

By WILLY VAN DRIESSCHE

From the Laboratorium voor Fysiologie, K.U.L. Campus Gasthuisberg, B-3000 Leuven, Belgium

SUMMARY

1. Basolateral membranes of the frog urinary bladder were investigated after increasing the cationic conductance of the apical membrane by the incorporation of nystatin.

2. K^+ currents were recorded in the presence of a mucosa to serosa oriented K^+ gradient (SO_4^{2-} Ringer solution). Nystatin caused a rapid rise of the short-circuit current (I_{sc}) followed by a slow increase over a period of 1–2 h.

3. Impedance analysis showed that the apical membrane resistance was drastically reduced by nystatin. The slow increase in I_{sc} was accompanied by a progressive increase in basolateral conductance.

4. The transepithelial current and conductance recorded in the presence of nystatin could be depressed with lidocaine added to the mucosal and serosal solution. The effects of lidocaine were completely reversible.

5. Noise analysis showed that lidocaine induced additional fluctuations in I_{sc}. The spectrum of these fluctuations was of the Lorentzian type. This noise component is caused by the random interruption of the current through the basolateral K^+ channels. The Lorentzian parameters were used to calculate the microscopic parameters of the basolateral K^+ channels.

INTRODUCTION

Already several decades ago, Koefoed-Johnsen & Ussing (1958) showed that the basolateral membranes of frog skin are mainly permeable to K^+. Since then, the K^+ conductance of the basolateral membranes in different epithelia has been the subject of numerous studies (Macknight, 1977). Electrophysiological studies of these membranes are difficult because of the complex structure of epithelia. Transepithelial electrical measurements will mostly reveal only indirect effects of alterations of the properties of the basolateral K^+ conductance on e.g. the apical Na^+ uptake and transepithelial Na^+ transport. Moreover, micro-electrode experiments showed that most of the resistance of the transcellular pathway is localized in the apical membrane (Helman & Fisher, 1977; Nagel & Essig, 1982). Therefore, electrical signals from the basolateral membrane will be strongly attenuated by the presence of the apical membranes in series with the basolateral signal source. Therefore, the

measurement of K^+ currents through the basolateral membranes is not possible with transepithelial voltage-clamp experiments.

To overcome such difficulties the pore-forming antibiotics nystatin, amphotericin B and gramicidin D have been employed to reduce the resistance of the apical barrier and to access the properties of the basolateral membranes (Wills, 1981). Lichtenstein & Leaf (1965) and Sharp, Coggins, Lichtenstein & Leaf (1966) used amphotericin B in studies of Na^+ transport through the toad urinary bladder. Nielsen (1977) employed the filipin-treated frog skin to access the basolateral Na^+–K^+-ATPase. On the other hand, Lewis, Eaton, Clausen & Diamond (1977) used nystatin to study the latter transport system in the rabbit urinary bladder, while Halm & Dawson (1983) employed amphotericin B for this purpose. The pore-forming antibiotics were also utilized in electrophysiological and radiotracer studies of the passive K^+ conductance of basolateral membranes of the rabbit urinary bladder (Lewis *et al.* 1977; Lewis & Wills, 1982), rabbit colon (Wills, Lewis & Eaton, 1979; Wills, Eaton, Lewis & Ifshin, 1979), toad urinary bladder (Garty, 1984) and turtle colon (Kirk & Dawson, 1983). These studies demonstrated that after treatment of the mucosal barrier with the antibiotics, most of the transcellular resistance resides in the basolateral membrane.

Recently we used the nystatin treatment to investigate the basolateral K^+ channels in the skin of the larval frog with fluctuation analysis (Hillyard & Van Driessche, 1984; Van Driessche & Hillyard, 1985). This study demonstrated that the conductance of the K^+-selective pathway in the basolateral membrane was depressed by quinidine.

In the present study we used the nystatin-treated epithelium of the frog urinary bladder to study the interaction of lidocaine with the basolateral K^+ channels. It is well known that lidocaine and its derivatives occlude different channel types: acetylcholine receptor channels are reversibly blocked by lidocaine (Neher & Steinbach, 1978; Adams, 1981) and the propagation of action potentials is blocked by the occlusion of Na^+ channels (Hille, 1984). Neher & Steinbach (1978) showed that the interaction of the drug with acetylcholine receptor channels induces additional flickering of the channel. These random interruptions of the single channel currents produce fluctuation of the macroscopic currents. This study demonstrates that lidocaine is also a very potent blocker of the basolateral K^+ conductance which is probably associated with cell swelling. We also show that lidocaine induces additional fluctuations of the current through the basolateral K^+ channels and can therefore be used as a probe for the study of single channel parameters with noise analysis. Compared to quinidine, the use of lidocaine turned out to have the advantages of a better reversibility of the K^+ current and conductance depression, a more favourable frequency range for the noise analysis and probably less secondary effects on the K^+ conductance. Contrary to Ba^{2+}, this probe can be used to study K^+ channels in SO_4^{2-}-Ringer solutions, a requirement for many studies in which cell swelling is restricted.

<div align="center">METHODS</div>

Preparation and solutions

The animals (*Rana catesbeiana*) were anaesthetized by exposure to an aqueous solution which contained 0·1 % (w/v) MS-222 (ethyl *m*-aminobenzoate; Sandoz, Bazel). The pH of this solution was adjusted to 7 by adding $NaHCO_3$. The urinary bladder was removed from the animal and small

pieces were glued (histoacryl blue, B. Braun Melsungen, F.R.G.) with its serosal surface on a lucite ring (inner diameter: 13·5 mm, outer diameter: 17·5 mm). In this way the tissue was immobilized and could be easily mounted in an Ussing-type chamber with negligible edge damage. The seal between the chamber and the tissue was achieved with silicon grease which was spread on the 2 mm width circular rim of the chamber (inner diameter: 8 mm). The distance between the two chamber halves was adjusted to avoid compression of the tissue. The surface in contact with the bathing solution measured 0·5 cm². Both sides of the tissue were continuously perfused with a flow rate of 8 ml/min. The volume of each chamber half was 1·35 ml. The voltage and current electrodes consisted of agar bridges, 1 M-KCl solution and the Ag-AgCl junction.

In order to reduce cell swelling after nystatin treatment, we used chloride-free solutions. Na^+-Ringer solution had the following composition: 57·6 mM-Na_2SO_4, 2·5 mM-$KHCO_3$ and 1 mM-$CaSO_4$ (pH = 8). K^+-Ringer solution has a similar composition to Na^+-Ringer solution with the exception of Na_2SO_4 which was replaced by K_2SO_4. The serosal surface was always exposed to Na^+-Ringer solution while the mucosal side was mostly in contact with K^+-Ringer solution. Nystatin (Sigma, St. Louis, MO, U.S.A.) was dissolved in dimethylsulphoxide (600000 u/ml) and added to the K^+-Ringer solution used as mucosal solution. The final concentration of the antibiotic in the mucosal compartment was 100 u/ml. Lidocaine hydrochloride (Federa, Brussels, Belgium) was dissolved in water (5×10^{-2} M) and aliquots of this stock solution were added to the mucosal and serosal solutions. Noise data, the macroscopic current and conductance were recorded at seven different lidocaine concentrations: 10, 25, 50, 75, 100, 150 and 200 μM.

Macroscopic electrical parameters

The depression of the short-circuit current (I_{sc}) by lidocaine was analysed with the direct linear plot method as proposed by Eisenthal & Cornish-Bowden (1974). If the inhibition of I_{sc} fulfils Michaelis–Menten kinetics, the reduction of I_{sc} (ΔI_{sc}) by lidocaine can be described by the following relationships:

$$\Delta I_{sc} = I_{sc}^c - I_{sc}^{LID} = \frac{I_{max}^{LID}}{1 + K_{LID}^{mac}/[LID]}, \qquad (1)$$

where I_{max}^{LID} is the licocaine-blockable current, I_{sc}^c, the control I_{sc} recorded in the absence of lidocaine, I_{sc}^{LID}, the I_{sc} recorded in the presence of lidocaine and K_{LID}^{mac}, the lidocaine concentration required to block 50 % of I_{max}^{LID}. After re-arranging eqn. (1) we obtain:

$$\frac{I_{max}^{LID}}{\Delta I_{sc}} - \frac{K_{LID}^{mac}}{[LID]} = 1. \qquad (2)$$

According to the direct linear plot method the parameters I_{max}^{LID} and K_{LID}^{mac} are considered as variables while ΔI_{sc} and [LID] are used as constants. For each measurement of ΔI_{sc} at a certain [LID], there exists a linear relationship between I_{max}^{LID} and K_{LID}^{mac}. This relation is represented by a straight line in a $I_{max}^{LID} - K_{LID}^{mac}$ plot with $-$[LID] and ΔI_{sc} as intercepts with the abcissa and ordinate, respectively. The coordinates of the intersections of these linear relations constitute estimates of K_{LID}^{mac} and I_{max}^{LID}. The median of these estimates was used as the best estimate for K_{LID}^{mac} and I_{max}^{LID}. Further details of this analysis are described in a previous report (Van Driessche & Erlij, 1983).

The transepithelial potential and current were monitored with a low-noise voltage-clamp device which was described previously (Van Driessche & Lindemann, 1978). The transepithelial potential was continuously clamped to 0 mV and the transepithelial conductance (G_t) was measured by clamping the potential to 10 mV during 1–2 s. I_{sc} was continuously recorded on a standard X–T recorder (see Fig. 1). The G_t measurements caused brief current deflexions as seen in Fig. 1. The measurement of this conductance was done with a digital voltmeter. The frequency response of the voltage-clamp circuit was checked by applying a square wave voltage to the command input of the feed-back amplifier. The closed-loop gain was adjusted while the voltage and current signals from the voltage clamp were monitored on an oscilloscope. This procedure also allowed us to inspect the capacitive transients in the current responses to the square-wave pulses. The absence of these capacitive current transients is indicative of eventual damage to the preparation.

Noise analysis

The transepithelial current was amplified with an a.c. coupled amplifier with a gain of 1000. The fluctuation in current was analysed with a Fourier analyser system which was constructed with

SBC computer boards (INTEL) (Van Driessche & Erlij, 1983). As previously (Van Driessche & Erlij, 1983) three spectra of 256 frequence lines were recorded simultaneously with fundamental frequencies of 0·2, 0·8 and 3·2 Hz, respectively. The spectra calculated from 30 sweeps were averaged and merged. The number of data points was reduced by averaging the spectral data contained in an interval of 1/8 of an octave on the frequency axis (see Fig. 6).

The recorded spectra contained mostly a low-frequency noise component. The dependence on frequency of this low-frequency component (S_B) can be described by the following equation:

$$S_B(f) = K_B/f^\alpha, \tag{3}$$

where K_B represents the power density at $f = 1$ Hz and α the slope of the straight line in a double-logarithmic representation. However, if the current is interrupted randomly by the opening and closing of channels, the spectrum of the fluctuation in the current contains a Lorentzian component (S_L) (Van Driessche & Zeiske, 1980):

$$S_L(f) = \frac{S_o}{1+(f/f_c)^2}, \tag{4}$$

where S_o (plateau value) is equal to the power density in the lower frequency limit and f_c (corner frequency) the frequency where the power density is equal to $S_o/2$. At the highest frequencies, the amplifier noise became dominant because of the decrease of the membrane impedance (Van Driessche & Lindemann, 1978; Van Driessche & Gullentops, 1982). This high frequency part of the spectrum was omitted in the further analysis of the data. The remaining lower and middle part of the spectra was used to determine the Lorentzian parameters (S_o and f_c) and the parameters of the low-frequency component (K_B and α). For that purpose we used non-linear regression analysis to fit the sum of eqns. (3) and (4):

$$S(f) = S_B(f) + S_L(f), \tag{5}$$

to the data points (Van Driessche & Zeiske, 1980).

Impedance measurements

A sequence of psuedo-random binary noise pulses of 16384 length was generated by a digital circuit and used as the command signal for the voltage-clamp device. The clock pulses which were used for the shift registers of the pseudo-random noise generator were synchronous with the clock of the analog-to-digital converter system used for data sampling. In this way the length of the pseudo-random binary noise sequence (p.r.b.n.s.) was identical to the length of the window used for the Fourier analysis. The p.r.b.n.s. was filtered with a 36 dB/octave Butterworth low-pass filter (Difa Benelux, Breda, Netherlands) with a cut-off frequency which was equal to 90 % of the Nyquist frequency of the Fourier analysis. In this way the spectral components which were not analysed were removed from the command signal and the capacitive transients associated with square voltage pulses were drastically reduced. The p.r.b.n.s. was also filtered with a high-pass filter (12 dB/octave, cut-off frequency = 0·01 Hz) to remove the d.c. component of the command voltage. In this way the mean voltage across the preparation remained 0 mV. The peak-to-peak amplitude of the command signal was approximately 5 mV. The current and voltage signals from the voltage clamp were filtered with a 36 dB/octave Butterworth low-pass filter with a cut-off frequency equal to 85 % of the Nyquist frequency. 16384 data points of the current and voltage signal were sampled simultaneously. The Fourier transformed representation of the voltage and current signal was calculated by Fast Fourier Transformation as used for the noise analysis (Van Driessche & Erlij, 1983). The impedance function was calculated by dividing the transformed voltage and current signals. Only one sweep of the voltage and current signal was used. The impedance data at frequencies larger than 75 % of the Nyquist frequency were omitted for further analysis. The remaining 6144 frequency lines were subjected to data reduction by averaging the data contained in $\frac{1}{8}$ of an octave. The resulting impedance plot contained eighty-nine frequency lines (see Fig. 2).

Under conditions prior to the nystatin treatment, the electrical characteristics of the urinary bladder can be approximately described by the electrical impedance of a first-order system of which the electrical equivalent model consists of a simple parallel RC network with a series resistance (Clausen, Lewis & Diamond, 1979; Gögelein & Van Driessche, 1981). However, as generally found in biological tissues, the impedance locus consists of a semicircle with a 'depressed' centre, which

was attributed to distributed time constants (Clausen *et al.* 1979). The equivalent impedance can be described by the following expression (Cole & Cole, 1941):

$$Z = R_\mathrm{s} + \frac{R_\mathrm{m}}{1 + (jwR_\mathrm{m} C_\mathrm{m})^{1-\beta}}, \tag{6}$$

where R_m represents the equivalent parallel resistance, C_m the equivalent parallel capacitance and R_s the resistance in series with the R_m–C_m network. The angle β (in radians) is equal to $2\phi/\pi$, where ϕ is the angle (in degrees) between the real axis and the line which connects the centre of the semicircle with its intersections with the real axis. j and w have their usual meaning: $j = \sqrt{-1}$ and $w = 2\pi f$. R_s in the investigated system is approximately equal to the resistance of the bathing solutions between the voltage electrodes plus the resistance of the connective tissue. R_s can be directly obtained from the impedance plot as the section of the real axis between the origin and the left intersection with the semicircle. We could fit eqn. (6) to the impedance data obtained prior to nystatin treatment. This indicates that the impedance of only one membrane dominates. In this system the apical membrane has the highest resistance and the smallest capacitance and therefore the highest impedance over the entire frequency range. After the addition of nystatin to the mucosal medium, the low-frequency part of the impedance data could be fitted with eqn. (6). The deviation at higher frequencies is probably caused by the fact that the apical and basolateral membrane impedances have comparable magnitudes (see Results). We used the impedance measurements to get a rough estimate of the membrane capacitance before and after nystatin treatment. This analysis demonstrates that the apical membrane resistance was drastically reduced by nystatin and that secondly, the basolateral conductance increased. A more precise analysis of the impedance data can be done by using the distributed impedance model (Clausen *et al.* 1979). However the use of this model requires additional information including the voltage divider ratio obtained from micro-electrode studies.

The procedure for fitting eqn. (6) to the data was similar to the one used for fitting the noise spectra (see also Gögelein & Van Driessche, 1981). After nystatin treatment only impedance data from the low-frequency part were used to determine the equivalent membrane parameters.

If not mentioned differently, mean values are given ±S.E. of mean.

<div align="center">RESULTS</div>

I_sc and G_t before and after nystatin treatment

In previous experiments with the epithelium of the larval frog skin we showed that approximately 138 u. nystatin/ml were required to reduce the resistance of the apical membrane drastically (Hillyard & Van Driessche, 1984; Van Driessche & Hillyard, 1985). In the present studies with the urinary bladder of the frog, a smaller amount of the antibiotic was sufficient to increase drastically the conductance of the apical membrane. We used in our experiments a concentration of 100 u. nystatin/ml which was added to the mucosal K_2SO_4-Ringer solution while the serosal side was exposed to Na_2SO_4-Ringer solution. Because of the negligible conductance of the apical membrane for K^+ and the very small conductance and selectivity of the paracellular pathway of this preparation (Macknight, DiBona & Leaf, 1980), only a very small I_sc was recorded before the addition of nystatin: 1.05 ± 0.71 μA/cm² ($n = 8$). The mean value of the R_t recorded under these initial conditions was: 25.0 ± 7.1 kΩ cm².

The addition of nystatin to the mucosal solution caused an abrupt increase of I_sc and the G_t (Fig. 1). The mean value of I_sc recorded immediately after nystatin addition (peak value of I_sc recorded within 2 min after nystatin treatment: I_peak) was 9.1 ± 1.3 μA/cm² ($n = 8$). Concomitantly the R_t dropped to 2.8 ± 0.9 kΩ cm². It is reasonable to assume that the initial rise in I_sc and G_t are caused by the immediate incorporation of nystatin in the apical membrane. This is in agreement with findings of others (Wills, *et al.* 1979; Garty, 1984) who showed that nystatin facilitates the

movement of K^+ across the apical membrane. On the other hand, a slow increase of I_{sc} and G_t was always observed in the 1–2 h period following the addition of nystatin. Mostly, stable I_{sc} and G_t values were obtained after approximately 100 min exposure time to nystatin in the presence of the mucosa to serosa oriented K^+ gradient. The mean values for I_{sc} and R_t recorded after this long exposure were $I_{sc}^c = 87 \cdot 8 \pm 14 \cdot 4\ \mu A/cm^2$ ($n = 8$) and $R_t = 0 \cdot 64 \pm 0 \cdot 07\ k\Omega\ cm^2$. The increase of I_{sc} and G_t after long exposure could be caused either (a) by a further decrease of the apical membrane resistance by an increase in the amount of incorporated nystatin or (b) by secondary effects on the basolateral membrane conductance. In order to resolve this question we recorded the electrical impedance of the tissue before and at regular time intervals after the addition of nystatin. This method allows, under certain conditions, estimates of the apical and basolateral membrane resistances to be made.
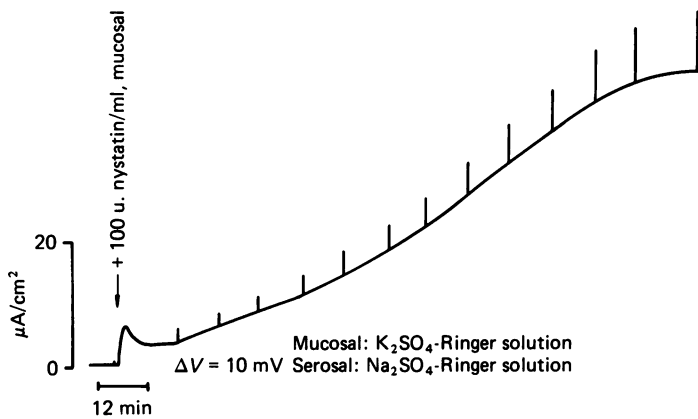

Fig. 1. Recording of the short-circuit current (I_{sc}) before and after addition of 100 u. nystatin/ml to the mucosal K_2SO_4-Ringer solution while the serosal medium consisted of Na_2SO_4-Ringer solution. The vertical deflexions are caused by imposing 10 mV pulses of about 1 s duration across the epithelium and are therefore proportional to the G_t. Note the peak in I_{sc} recorded immediately after the addition of nystatin (I_{peak}). I_{sc}^c denotes the plateau current recorded after long exposure to nystatin.

Impedance measurement

The transepithelial electrical impedance was measured while the mean voltage across the epithelium remained zero. Fig. 2A shows such an impedance function, represented in a Nyquist plot. It was recorded under control conditions before the addition of nystatin. A semicircle with depressed centre (eqn. (6), Methods) could be fitted through the data points. This suggests that a simple RC network can be used as an electrical equivalent model for the preparation. Such impedance functions are found in other biological membranes (Schanne & Ceretti, 1978). Studies of the electrical impedance of epithelia showed similar impedance plots for the rabbit urinary bladder (Clausen *et al.* 1979), frog skin (Brown & Kastella, 1965; Smith, 1971) and *Necturus* gallbladder (Gögelein & Van Driessche, 1981). From the fits of eqn. (6) we obtained the electrical equivalent parameters: $R_m = 17 \cdot 9 \pm 3 \cdot 0\ k\Omega\ cm^2$, and $C_m = 1 \cdot 56 \pm 0 \cdot 24\ \mu F/cm^2$. The angle ϕ which describes the depression of the centre of the semicircle was: $\phi = 8 \cdot 00 \pm 0 \cdot 42$ deg ($n = 7$). Similar values for ϕ and C_m were
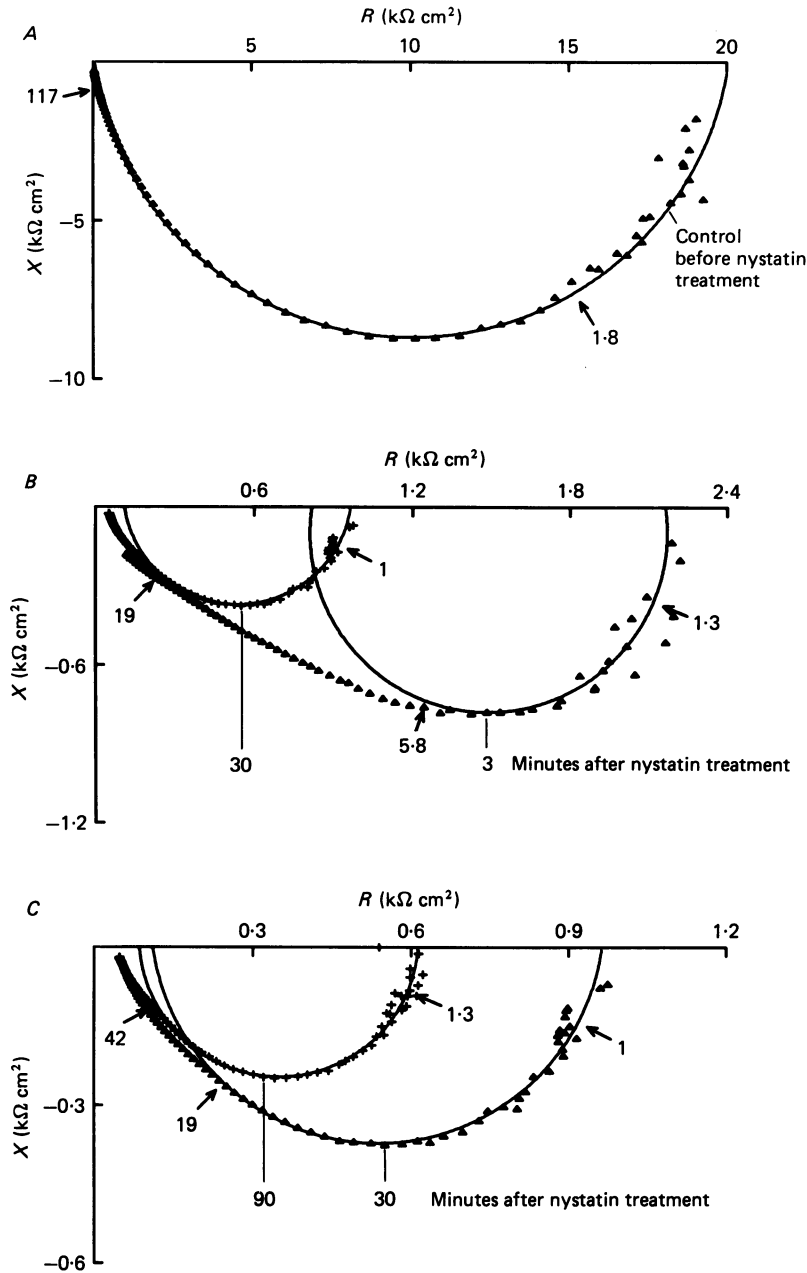
Fig. 2. Impedance measurements before and after the addition of nystatin represented in a Nyquist diagram. Abcissa: real part of the impedance (R); ordinate: imaginary part of the impedance (X). *A*, impedance recorded before the addition of nystatin. The continuous line is the best fit of eqn. (4) to the data points. Only the data points between the arrows were used in the fit procedure. The numbers at the arrows are the frequencies of the corresponding data points. *B*, impedance curves recorded 3 and 30 min after nystatin treatment. *C*, comparison of the impedance recorded 30 and 90 min after nystatin treatment.

found in other tissues (Schanne & Ceretti, 1978). The R_s with the equivalent RC network was: $R_s = 70\cdot8 \pm 13\cdot2$ kΩ cm^2. It is localized in the solution layer between the voltage electrodes and in the connective tissue. On the other hand, R_m is mainly determined by the resistance of the apical membrane and the paracellular pathway. Under the present control conditions (no Na$^+$ transport), the basolateral membrane has a much higher electrical conductance than the apical membrane. Also the capacitance of the basolateral membrane is much larger than the apical membrane capacitance because of the numerous infoldings of the former. Consequently, the apical membrane parameters (R_a and C_a) will determine the transepithelial impedance over the entire frequency range so that $R_a \approx R_m$ and $C_a \approx C_m$. A more accurate estimate of the membrane parameters could be obtained by using a distributed impedance model (Clausen *et al.* 1979) in combination with micro-electrode data.
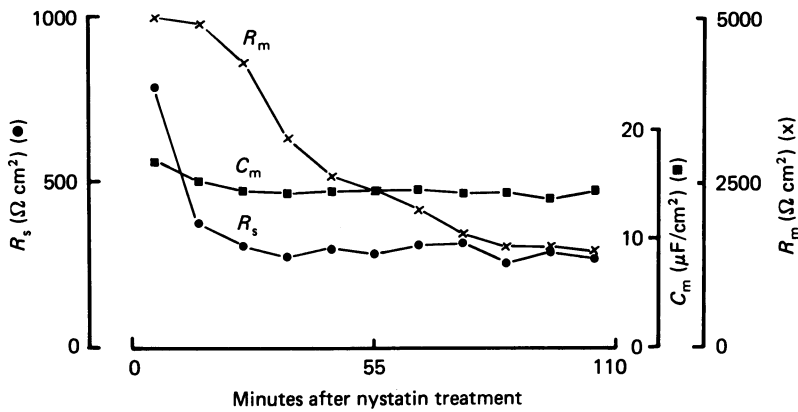

Fig. 3. Changes of the electrical equivalent parameters after the addition of nystatin (100 u./ml) to the mucosal K$_2$SO$_4$-Ringer solution. R_m represents the equivalent electrical resistance determined from impedance curves as in Fig. 2B and C. C_m is the electrical capacitance in parallel with R_m and R_s the series resistance. R_m and C_m are determined by the basolateral membrane characteristics, while R_s depends strongly on the apical membrane resistance. Before the addition of nystatin, the electrical equivalent parameters of the tissue, which are under these circumstances determined by the apical membrane, were: $R_m = 20\cdot3$ kΩ cm^2, $C_m = 1\cdot6$ μF/cm^2, $R_s = 60\cdot3$ Ω cm^2 and $\phi = 3\cdot9$ deg.

Panels B and C in Fig. 2 show the impedance data recorded 3, 30 and 90 min after the addition of nystatin, The impedance curve recorded immediately after the exposure to nystatin deviates strongly from the semicircular plot which was recorded under control conditions. However, if the data at the higher frequencies were omitted, the remaining low-frequency part could be fitted with eqn. (6). The deviation from eqn. (6) becomes smaller after longer exposure times (after 30 and 90 min). We recorded the impedance function at 10 min intervals after addition of nystatin. The electrical equivalent parameters obtained from fits of eqn. (6) to the low-frequency part of the data are demonstrated for a typical experiment in Fig. 3. In this experiment, the resistance of the preparation (R_m) dropped within 5 min after nystatin treatment from 25·86 to 5·02 kΩ cm^2. After this initial and rapid drop, R_m decreased further to reach a value of 1·34 kΩ cm^2 after 105 min. On the other hand, the electrical capacity of the preparation increased within 5 min from 1·26 to

16·8 μF/cm^2 and decreased only slightly to 15·0 μF/cm^2 in the following long exposure period. The resistance (R_s) in series with the capacitive network increased from 90 Ω cm^2 under control conditions to 830 Ω cm^2, 5 min after the addition of nystatin. In the following 10 min period R_s dropped to 340 Ω cm^2 and remained approximately unchanged during the rest of the experiment. The mean value of C_m recorded after 90 min of nystatin treatment was 17·7 $\pm$ 5·3 μF/cm^2 ($n = 5$) and for $R_m = 656 \pm 64$ Ω cm^2 ($n = 5$). In these five experiments, the resistance in series with the equivalent RC network was 128 $\pm$ 33 Ω cm^2. The basolateral membrane capacitance found agrees fairly well with the values obtained by Clausen *et al.* (1979) in the rabbit urinary bladder and using the distributed impedance model ($C_b/C_a \approx 12$).

These results can be understood by assuming the second hypothesis which was proposed above. Immediately after the addition of nystatin, the resistance of the preparation drops because of the increase of the permeability of the apical membrane. Concomitantly, the impedance of the basolateral membrane becomes dominant in the low-frequency region of the impedance plot. This is clear from the fact that the value of the capacitance is about 12 times larger than the C_m values obtained under control conditions. This is in agreement with observations of others in studies where the basolateral membrane impedance became visible in the impedance plot after increasing the basolateral membrane resistance (Smith, 1971). The resistance in series with the capacitance is however much larger than the series resistance recorded under control conditions. Prior to nystatin treatment (control), R_s is the series resistance of the whole preparation (apical + basolateral), while from the fits of the low-frequency part of the impedance after nystatin treatment, we obtain a R_s value which is predominantly determined by the remaining apical membrane resistance. An important decrease of this R_s value was observed in the period between 5 and 15 min after nystatin application (see Fig. 3). This is probably due to an increase of the number of nystatin channels which are incorporated in the apical membrane. After this initial period the resistance of the apical membrane (R_s in this case) remains approximately constant. On the other hand, the resistance of the basolateral membrane, which is assumed to be equal to the R_m value in parallel with C_m decreased continuously during the whole experiment. During the first 20 min following the nystatin addition, the decrease occurred rapidly, while afterwards a tendency to reach a plateau was visible. The reason for this gradual increase of the basolateral membrane conductance is not clear. However, it is conceivable that cell swelling occurs during the long exposure to nystatin. This phenomenon is known to induce an elevated K$^+$ permeability (Germann & Dawson, 1984) and in several other cell types (Grinstein, Rothstein, Sarkadi & Gelfand, 1984). However, cell swelling is generally assumed to occur when Cl$^-$-Ringer solution is used and avoided when the tissue is bathed with SO$_4$$^{2-}$-Ringer solution. Nevertheless, the increase in I_{sc} and G_t remained absent when the nystatin long exposure experiments were performed with gluconate-Ringer solution (own unpublished observation). Moreover if gluconate was partly replaced by Cl$^-$, a similar increase of I_{sc} and G_t after nystatin treatment was observed. Also when using hypertonic SO$_4$$^{2-}$-Ringer solution the long time increase of I_{sc} and G_t remained absent. Thus, it seems that the slow I_{sc} and G_t increases are related to cell swelling which occurs when the permeable anion is

present in the solutions. It is therefore conceivable that also in the experiments with SO_4^{2-}-Ringer solution cell swelling occurs after the addition of nystatin. This would require that the nystatin channels or the apical and/or basolateral membranes have a finite permeability for SO_4^{2-}. This hypothesis is also supported by the following observation: we observed in several experiments that after an exposure time of 150 min to nystatin, the R_t suddenly decreased to an extremely small value. Concomitantly the capacitance current transients which are induced by square-wave command voltage pulses (see Methods) could no longer be observed. Therefore, it seems that the abrupt resistance decrease is caused by tissue damage which is related to cell swelling. Similar observations of cell bursting were made by other investigators in experiments with Cl^--Ringer solution (Wills, 1981).

So far it is clear that nystatin rapidly decreases the apical membrane resistance which reaches a stable value after about 15 min. On the other hand, the basolateral membrane conductance increases over a period of at least 90 min. Therefore, even a slight tendency to increase this conductance is still present. It cannot be excluded that a fraction of the increase in basolateral membrane conductance is due to the diffusion of nystatin into the cells or incorporation into the basolateral membranes. However, such an additional unselective pathway would not lead to the observed current increase which seems to be purely carried by K^+. The latter is shown in the next section by the complete blockade of this current component by lidocaine.

Inhibition of I_{sc} by lidocaine

In previous experiments with the epithelium of the larval frog skin (Hillyard & Van Driessche, 1984; Van Driessche & Hillyard, 1985) we showed that quinidine blocks basolateral K^+ channels. A similar conclusion was made from studies with the intact frog skin (Abramcheck, Van Driessche & Helman, 1985). Recently we reported that quinidine and lidocaine inhibit basolateral K^+ conductance (Van Driessche, Hillyard & Cantiello, 1985). In the present study we chose to use lidocaine because of its better reversibility compared to quinine and quinidine. Lidocaine was added to both sides of the preparation in order to achieve a well-defined concentration of lidocaine at the site of action. A single side application of lidocaine would create a steep concentration gradient for lidocaine in the tissue. This gradient would depend strongly on the wash-out at the opposite side of the tissue which depends on several parameters, including, length of the diffusion path and the flow rate of the perfusing solutions. A detailed analysis of this problem was made in a previous study when using quinidine to block basolateral K^+ channels (Van Driessche & Hillyard, 1985). Fig. 4 shows the effect of lidocaine on the I_{sc} recorded after increasing the apical conductance with nystatin. A gradual increase of the lidocaine concentration in the mucosal and serosal solutions from 10 to 200 μM caused a dose-dependent inhibition of the I_{sc}. Concomitantly, the G_t decreased. The mean value of I_{sc} recorded after nystatin addition 87.4 ± 4.4 μA/cm^2 was depressed to 19.4 ± 2.9 μA/cm^2 ($n = 8$) when 200 μM-lidocaine was present in both chamber compartments. The R_t increased from 0.64 ± 0.07 to 1.49 ± 0.36 kΩ cm^2. After removing lidocaine from both bathing solutions, I_{sc} increased rapidly and became generally larger than the control value. This overshoot might at least be partially caused by a further increase of the basolateral conductance during the lidocaine treatment. Nevertheless we tested if

the inhibition of I_{sc} obeyed Michaelis–Menten kinetics. We used the direct linear method, described in the Method section, to estimate the dose needed for the inhibition of 50 % of the current, K_{LID}^{mac} and the maximum lidocaine blockable component of I_{sc}, I_{max}^{LID}. A typical example is shown in Fig. 5. The coordinates of the intersections are estimates of I_{max}^{LID} (ordinate) and K_{LID}^{mac} (abcissa). The mean value of K_{LID}^{mac} was $38\cdot0\pm2\cdot3$ μM ($n = 7$).
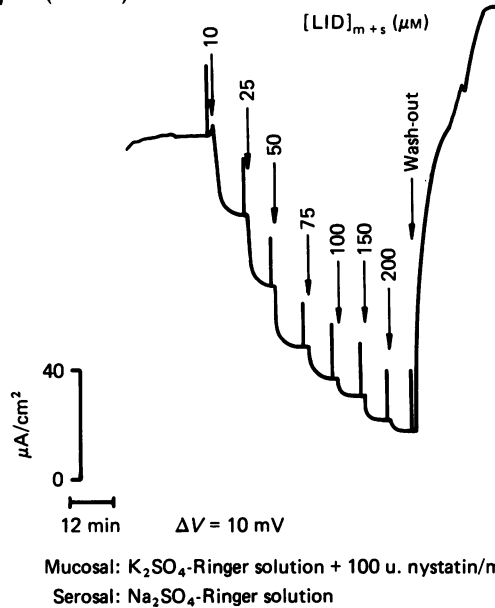

Fig. 4. Inhibition of the transepithelial current recorded after long exposure to nystatin. The lidocaine concentration in the mucosal and serosal compartment ($[LID]_{m+s}$) was gradually increased from 10 to 200 μM. The vertical deflexions are proportional to the G_t and are caused by clamping the transepithelial potential at 10 mV.
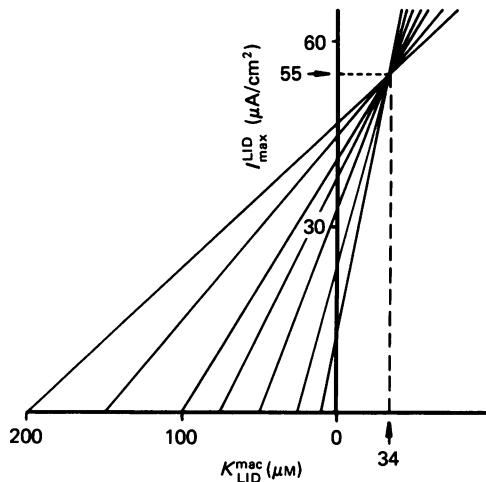

Fig. 5. Example of the estimation of the Michaelis–Menten constant (K_{LID}^{mac}) and the lidocaine-blockable current (I_{max}^{LID}) by the direct linear plot method. In the example shown $I_{max}^{LID} = 55$ μA/cm^2 and $K_{LID}^{mac} = 34$ μM.

Recently, Germann & Dawson (1984) suggested that the K^+ conductance which is caused by cell swelling is blockable by quinidine, while the native K^+ permeability is not sensitive to this blocker. To test this hypothesis on our data we compared the amount of current which is not blockable by lidocaine with the initial peak current recorded immediately after the addition of nystatin (see Fig. 1). The amount of lidocaine-blockable current calculated as the percentage of control ($100 \times I_{max}^{LID}/I_{sc}^{c}$), was $92 \cdot 7 \pm 4 \cdot 2 \%$ ($n = 7$). Consequently, $7 \cdot 3 \%$ of the I_{sc} is insensitive to lidocaine. We compared this result with the peak current (I_{peak} recorded immediately after the addition of nystatin, see Fig. 1). The mean value of this peak current was $13 \cdot 5 \pm 3 \cdot 6 \ \mu A/cm^2$ ($n = 7$). The ratio of I_{peak} to I_{sc}^{c} (I_{sc} after long exposure to nystatin) was $16 \cdot 5 \pm 4 \cdot 3 \%$. Consequently, it seems that lidocaine also blocks partially the 'native' K^+ current which arises immediately after the addition of nystatin. It is however possible that this discrepancy is caused by errors in the estimation of I_{max}^{LID} as a consequence of the continuous slow rise in I_{sc}, even during recording of the lidocaine dose–response curves. Therefore it might still be that lidocaine, like quinidine in turtle colon, inhibits only the K^+ conductance which is associated with cell swelling (Germann & Dawson, 1984).

Fluctuation analysis

We analysed the fluctuation in current after the treatment of the apical surface with nystatin, prior to lidocaine and in the presence of different lidocaine concentrations in the bathing media (Fig. 6).

Spontaneous current fluctuations. The spectra recorded after nystatin treatment (Fig. 6A) were slightly curved which suggested the presence of a Lorentzian component which is related to current interruptions caused by channels which open and close randomly. Until now it has not been possible to localize unequivocally the source of this noise component. In previous studies (Van Driessche, Wills, Hillyard & Zeiske, 1982) we suggested that these fluctuations are caused by the random interruption of the K^+ current by the basolateral K^+ channels. It can, however, not be excluded that the fluctuations arise from the random opening and closing of the nystatin channels. However, the conductance fluctuations which originate from the nystatin channels would be strongly attenuated because the basolateral membrane constitutes a large series resistance for the apical membrane (Van Driessche & Gögelein, 1980; Van Driessche & Gullentops, 1982). The relation between the transepithelial fluctuation in I_{sc} (S_I^{tr}) and the fluctuation expected if a perfect voltage clamp across the apical membrane were applied (S_I^{ap}) was derived previously (Van Driessche & Gögelein, 1980):

$$S_I^{tr} (f) = S_I^{ap}(f) \cdot |H(f)|^2. \qquad (7)$$

At the lower frequency limit the attenuation factor ($H(f)$) simplifies to

$$H(0) = \frac{R_a}{R_a + R_b}. \qquad (8)$$

The values of R_a and R_b were estimated from the impedance measurements. It is clear from the analysis discussed in section B that the apical membrane resistance is maximally equal to the R_s obtained from the impedance analysis after nystatin
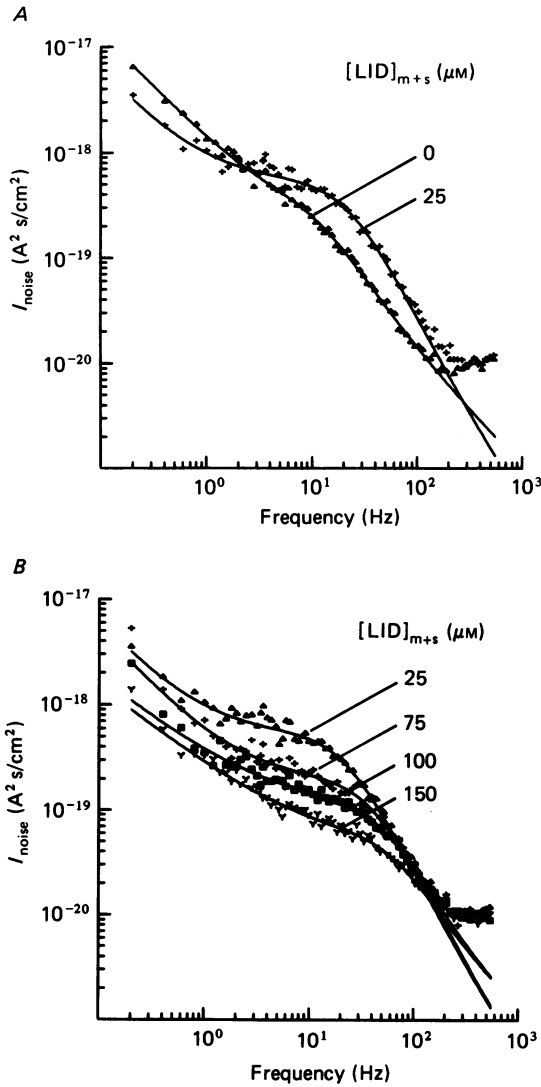
Fig. 6. Spectra recorded by fluctuation analysis. Before lidocaine was added to the bathing solutions ($[\text{LID}]_{\text{m+s}}$, the lidocaine concentration in the mucosal and serosal compartments), a Lorentzian component was visible in the power density spectra (spontaneous Lorentzian). In the presence of lidocaine (25–150 μM), blocker-induced fluctuations produced the Lorentzian noise in the power density spectra.

treatment. Mean values for R_{a} and R_{b} thus estimated were $R_{\text{a}} \approx R_{\text{s}} = 120 \pm 29\ \Omega\ \text{cm}^2$ and $R_{\text{b}} \approx R_{\text{m}} = 656 \pm 74\ \Omega\ \text{cm}^2$. Using these values we calculated $H(0) = 0.15$ and $S_I^{\text{tr}} = 0.024 \cdot S_I^{\text{ap}}$. Using this correction factor for the plateau values which were recorded transepithelially $202 \pm 49 \times 10^{-21}\ \text{A}^2\ \text{s}/\text{cm}^2$ we obtain: $S_I^{\text{ap}} = 8.4 \pm 2.0 \times 10^{-18}\ \text{A}^2\ \text{s}/\text{cm}^2$ ($n = 5$). Although this plateau value is very large, we cannot exclude the possibility that the spontaneous Lorentzian component is caused by current interruptions through nystatin channels in the apical membrane.

Blocker-induced fluctuations. It is well known that the current which is depressed by a reversible blocker contains fluctuations which are caused by the random interaction of the blocker with its receptor. This was found previously for the amiloride-inhibited Na^+ current (Lindemann & Van Driessche, 1977; Van Driessche & Erlij, 1983) the interaction of Ba^{2+} with the apical K^+ channel (Van Driessche & Zeiske, 1980) and more recently for the blockage of the K^+ current through basolateral K^+ channels of the tadpole skin epithelium (Hillyard & Van Driessche, 1984: Van Driessche & Hillyard, 1985). The analysis of the fluctuation of the I_{sc} which is depressed by the blocker reveals a Lorentzian component in the power density spectrum. This was also found in the present experiments when we analysed the fluctuations of the lidocaine-depressed current (Fig. 6). In Fig. 6A we compare the spectra recorded in the absence of lidocaine with a spectrum recorded after the addition of 25 μM-lidocaine to both sides. In the presence of 25 μM-lidocaine the low-frequency fluctuations were slightly depressed while in the high-frequency part the intensities were larger than under control conditions. A Lorentzian component could be fitted to the spectral data. When the lidocaine concentration was raised (Fig. 6B), the Lorentzian plateau was depressed and the corner frequency shifted towards higher frequencies. The corner frequencies were plotted as a function of the lidocaine concentration ([LID]) (Fig. 7). The linear relation between $2\pi f_c$ and [LID] suggests pseudo-first-order kinetics for the lidocaine-receptor interaction. The on- (k_{01}) and off-rate (k_{10}) for blocker-receptor interaction can be determined from linear regression analysis of the data in Fig. 7 with the following relation:

$$2\pi f_c = k_{01} \cdot [LID] + k_{10}. \tag{9}$$

In this way, we obtained: $k_{01} = 2 \cdot 4 \pm 0 \cdot 2 \ \mu M^{-1} \ s^{-1}$ and $k_{10} = 98 \cdot 7 \pm 15 \cdot 4 \ s^{-1}$ (mean $\pm$ S.D.). The Michaelis–Menten constant of the lidocaine–receptor system is equal to the ratio of the rate constants: $K_{LID}^{mic} = k_{10}/k_{01}$ which was in this series of experiments: $41 \cdot 2 \pm 6 \cdot 9 \ \mu M$ (mean $\pm$ S.D.). This value is very close to the K_{LID}^{mac} which we obtained from the inhibition of the I_{sc}. Consequently, it is very likely that the macroscopic inhibition of I_{sc} fulfils Michaelis–Menten kinetics. Using the rate constants (k_{01} and k_{10}) the I_{sc} data and the S_0 values, we calculated the single channel currents (i_K) with the following expression (Van Driessche & Zeiske, 1980):

$$i_K = \frac{S_0 \cdot \pi^2 \cdot f_c^2}{I_K \cdot k_{01} \cdot [LID]}. \tag{10}$$

I_K is the lidocaine-blockable current which we calculated as: $I_K = I_{sc}^{LID} - (I_{sc}^c - I_{max}^{LID})$ (see Methods). In this way we corrected the I_{sc} value for the lidocaine-insensitive current component. i_K was calculated from data obtained at seven lidocaine concentrations (from 10 to 200 μM, see Methods) from seven bladders. Forty-two spectra could be fitted. Two experiments had to be interrupted because of cell damage, probably caused by cell swelling (see above). As mean value we obtained $i_K = 1 \cdot 16 \pm 0 \cdot 13$ pA ($n = 42$). Also the channel density (M) was calculated as previously described (Van Driessche & Zeiske, 1980):

$$M = \frac{I_k \cdot 2\pi f_c}{i_K \cdot k_{10}}. \tag{11}$$

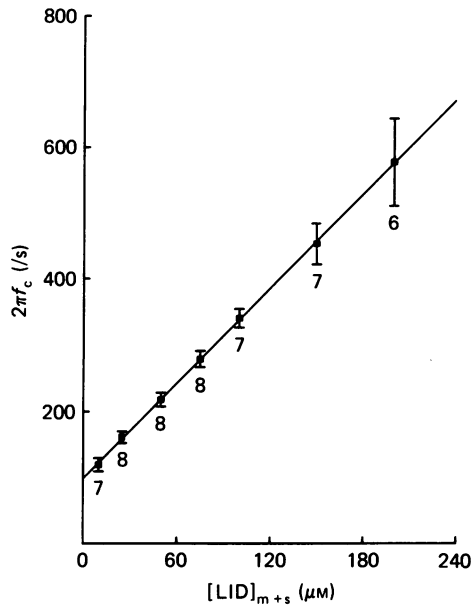We obtained: $M = 1 \cdot 20 \pm 0 \cdot 18 / \mu m^2$.

Fig. 7. Relation between the corner frequency and the lidocaine concentration in the mucosal and serosal compartment ($[LID]_{m+s}$). From linear regression analysis we obtained the on-rate (slope) and off-rate (ordinate intercept) of the blocker-receptor reaction (see text). The number of observations is indicated next to the symbols.

DISCUSSION

Nature of the I_{sc} recorded after nystatin treatment

Previously it has been shown by Garty (1984) that the nystatin-treated epithelium of the amphibian urinary bladder is an excellent system for the study of basolateral K^+ channel characteristics. These experiments as well as the present study were done in SO_4^{2-}-Ringer solution to avoid cell swelling and to maintain the integrity of the tissue. Thus, Garty (1984) reported that the prolonged exposure to nystatin did not cause a progressive G_t increase during a long exposure nor cell swelling. Contrary, we found that the G_t and the transepithelial K^+ current increased continuously over a period of at least 100 min. Most of this transepithelial current could be blocked by lidocaine (92 %). On the other hand, 84 % of this current was induced by the long exposure to nystatin. Consequently, at least the K^+ conductive pathway which was created by the prolonged exposure to nystatin was blockable by lidocaine. Contrary to the general accepted opinion we suggest that the nystatin channels or the apical and/or basolateral membranes have a finite permeability for SO_4^{2-}. Assuming this hypothesis, the slow increase in K^+ conductance, can be understood by cell swelling which is known to induce K^+ permeability in turtle colon (Germann & Dawson, 1984) and other cell types (Grinstein *et al.* 1984). This increase in cell volume should then be caused by the entry of K^+ into the cells through the nystatin channels followed by SO_4^{2-}. The increase of the K^+ conductance is rather slow in SO_4^{2-}-Ringer solution, while a rapid rise in K^+ conductance and current was found when Cl^--Ringer solution was used in studies with different epithelia (Lewis *et al.* 1977; Germann & Dawson, 1984). This difference in time course is probably related to the differences in

permeability of the nystatin channels or cell membranes between SO_4^{2-} and Cl^-. On the other hand, it must be kept in mind that the exposure of the intact epithelium to SO_4^{2-}-Ringer solution will cause a shrinkage of the cells. It is conceivable that the slow increase in K^+ conductance is partially associated with the recovery of the cell volume after nystatin treatment. The hypothesis that the lidocaine-blockable current was associated with cell swelling is supported by observations in similar epithelia (Germann & Dawson, 1984): experiments with the turtle colon showed that the K^+ current induced by cell swelling which occurred after amphothericin treatment in Cl^--Ringer solution could be blocked by quinidine which has similar effects on the K^+ conductance as lidocaine (Van Driessche et al. 1985). On the other hand these studies showed that the native K^+ conductance was insensitive to quinidine.

Reduction of the apical membrane resistance by nystatin

The increase of the G_t after the exposure of the apical membrane to nystatin was indicative for the reduction of the apical membrane resistance. Other studies with micro-electrodes (Lewis et al. 1977), demonstrated that the resistance of the apical barrier of rabbit urinary bladder was drastically reduced by nystatin.

In the present study we used impedance measurements to show that the apical membrane resistance is drastically reduced by nystatin. Clausen et al. (1979) made similar observations in studies with the rabbit urinary bladder. Moreover we could follow the changes in apical and basolateral membrane resistance during the long exposure to nystatin. This clearly demonstrated that most of the basolateral K^+ conductance was developed during this period and is probably related to changes in cell volume or cell composition.

The impedance measurements also showed that the intact epithelium behaves approximately like a simple RC network. Because of the high resistance of the apical membrane under non-transporting conditions, it is likely that the equivalent capacitance and resistance are approximately determined by the characteristics of the apical membrane. Similar values for the equivalent capacitance were found by others (Schifferdecker & Frömter, 1978). It is also clear that the value of C_m will depend on the degree of stretching of the tissue (Clausen et al. 1979). Measurements of the transepithelial impedance of the intact epithelium do not allow an estimate of the basolateral capacitance: mostly the apical membrane impedance dominates and because of the smaller resistance and larger capacitance of the basolateral membrane, the time constants are of the same order of magnitude. Therefore, the combined impedance of apical and basolateral membrane will give approximately a semicircle in the Nyquist plot. After nystatin treatment, however, the separation of the time constants of the apical and basolateral membrane becomes more pronounced. Therefore the contribution of apical membrane impedance will become visible in the high-frequency range while the basolateral membrane impedance will dominate on the low-frequency range.

K^+ channel blockage by lidocaine

This study showed that lidocaine (a) depresses the inward oriented current through the nystatin-treated epithelium (b) raises concomitantly the resistance of the preparation, and (c) induces additional fluctuation of I_{sc}. These findings suggest

that the local anaesthetic is a reversible blocker of basolateral K^+ channels. The interaction of lidocaine and its derivatives with the acetylcholine receptor channel has been extensively studied (Neher & Steinbach, 1978; Adams 1981). Also the action of lidocaine on Na^+ channels in excitable membranes has been the subject of many studies (Hille, 1984). However, the ability of this compound to block epithelial K^+ channels was not described before. Because lidocaine is very lipid soluble and therefore able to cross cell membranes easily, the action on the basolateral K^+ channels is very rapid. Because of its large permeability a constant concentration of the compound in the vicinity of the channel can only be achieved when it is added to both compartments (Van Driessche & Hillyard, 1985). This is especially the case in our chamber where both sides of the tissue are continuously perfused with fresh solutions. Another uncertainty in our analysis is the concentration of the active form of the compound: the uncharged base is very lipid soluble and equilibrates rapidly with the protonated form (Hille, 1984). It is presently unknown, which form interacts with the basolateral K^+ channels. However, comparison of the interaction of the drug with other channel types suggest that the ionized form binds to the receptor of the channel. The uncertainty on the concentration of this active form will effect the estimation of the on-rate. However, as discussed in previous papers, the errors in k_{10} and [LID] in eqn. (10) will cancel and therefore do not affect the values calculated for i_K and M. The single channel currents (≈ 1 pA) were very close to the values found for the apical K^+ channels in frog skin. However, comparison of the K^+ channel characteristics like single channel conductance is more difficult because of the uncertainty about the driving force for K^+ across the channel.

REFERENCES

ABRAMCHECK, F. J., VAN DRIESSCHE, W. & HELMAN, S. I. (1985). Autoregulation of apical membrane Na^+ permeability of tight epithelia. Noise analysis with amiloride and CGS 4270. *Journal of General Physiology* **85**, 555–582.

ADAMS, P. R. (1981). Acetylcholine receptor kinetics. *Journal of Membrane Biology* **58**, 161–174.

BROWN, A. C. & KASTELLA, K. G. (1965). The AC impedance of frog skin and its relation to active transport. *Biophysical Journal* **5**, 591–606.

CLAUSEN, C., LEWIS, S. A. & DIAMOND, J. M. (1979). Impedance analysis of a tight epithelium using a distributed resistance model. *Biophysical Journal* **26**, 291–318.

COLE, K. S. & COLE, R. H. (1941). Dispersion and absorption in dielectrics. I. Alternating current characteristics. *Journal of Chemical Physics* **9**, 341–351.

EISENTHAL, R. & CORNISH-BOWDEN, A. (1974). The direct linear plot. A new graphical procedure for estimating enzyme kinetic parameters. *Biochemical Journal* **139**, 715–720.

GARTY, H. (1984). Current–voltage relations of the basolateral membrane in tight amphibian epithelia: use of Nystatin to depolarize the apical membrane. *Journal of Membrane Biology* **77**, 213–222.

GERMANN, W. J. & DAWSON, D. C. (1984). Quinidine-sensitive basolateral potassium conductance in turtle colon: activation by cell swelling? *Federation Proceedings* **43**, 892.

GÖGELEIN, H. & VAN DRIESSCHE, W. (1981). Capacitive and inductive low frequency impedances of *Necturus* gallbladder epithelium. *Pflügers Archiv* **389**, 105–113.

GRINSTEIN, S., ROTHSTEIN, A., SARKADI, B. & GELFAND, E. W. (1984). Responses of lymphocytes to anisotonic media: volume-regulating behavior. *American Journal of Physiology* **246**, C204–215.

HALM, D. R. & DAWSON, D. C. (1983). Cation activation of the basolateral sodium-potassium pump in turtle colon. *Journal of General Physiology* **82**, 315–329.

HELMAN, S. I. & FISHER, R. S. (1977). Microelectrode studies of the active Na transport pathway of frog skin. *Journal of General Physiology* **69**, 571–604.

HILLE, B. (1984). *Ionic Channels of Excitable Membranes*. Sunderland, MA: Sinauer Associates Inc.

HILLYARD, S. D. & VAN DRIESSCHE, W. (1984). Quinidine blocks basolateral K$^+$ channels in tadpole skin. *Archives internationales de physiologie et de biochimie* **92**, P23–24.

KIRK, K. L. & DAWSON, D. C. (1983). Basolateral potassium channel in turtle colon. Evidence for single-file ion flow. *Journal of General Physiology* **82**, 297–313.

KOEFOED-JOHNSEN, V. & USSING, H. H. (1958). The nature of the frog skin potential. *Acta physiologica scandinavica* **42**, 298–308.

LEWIS, S. A., EATON, D. C., CLAUSEN, C. & DIAMOND, J. M. (1977). Nystatin as a probe for investigating the electrical properties of a tight epithelium. *Journal of General Physiology* **70**, 427–440.

LEWIS, S. A. & WILLS, N. K. (1982). Electrical properties of the rabbit urinary bladder assessed using gramicidin D. *Journal of Membrane Biology* **67**, 45–53.

LICHTENSTEIN, N. S. & LEAF, A. (1965). Effect of amphotericin B on the permeability of the toad bladder. *Journal of Clinical Investigation* **44**, 1328–1342.

LINDEMANN, B. & VAN DRIESSCHE, W. (1977). Sodium-specific membrane channels of frog skin are pores: current fluctuations reveal high turnover. *Science* **195**, 292–294.

MACKNIGHT, A. D. C. (1977). Epithelial transport of potassium. *Kidney International* **11**, 391–414.

MACKNIGHT, A. D. C., DIBONA, D. R. & LEAF, A. (1980). Sodium transport across toad urinary bladder: a model 'tight' epithelium. *Physiological Reviews* **60**, 615–715.

NAGEL, W. & ESSIG, A. (1982). Relationship of transepithelial electric potential to membrane potentials and conductance ratios in frog skin. *Journal of Membrane Biology* **69**, 125–136.

NEHER, E. & STEINBACH, J. H. (1978). Local anaesthetics transiently block currents through single acetylcholine-receptor channels. *Journal of Physiology* **277**, 153–176.

NIELSEN, R. (1977). Effect of the polyene antibiotic filipin on the permeability of inward- and outward-facing membrane of the isolated frog skin. *Acta physiologica scandinavica* **99**, 399–411.

SCHANNE, O. F. & CERETTI, E. R. P. (1978). *Impedance Measurements in Biological Cells*. New York, Chichester, Brisbane, Toronto: John Wiley & Sons.

SCHIFFERDECKER, E. & FRÖMTER, E. (1978). The AC impedance of *Necturus* gallbladder epithelium. *Pflügers Archiv* **177**, 125–133.

SHARP, G. W. G., COGGINS, C. H., LICHTENSTEIN, N. S. & LEAF, A. (1966). Evidence for a mucosal effect of aldosterone on sodium transport in the toad bladder. *Journal of Clinical Investigation* **45**, 1640–1647.

SMITH, P. G. (1971). The low-frequency electrical impedance of the isolated frog skin. *Acta physiologica scandinavica* **81**, 355–366.

VAN DRIESSCHE, W. & ERLIJ, D. (1983). Noise analysis of inward and outward Na$^+$ currents across the apical border of ouabain-treated frog skin. *Pflügers Archiv* **398**, 179–188.

VAN DRIESSCHE, W. & GÖGELEIN, H. (1980). Attenuation of current and voltage noise signals recorded from epithelia. *Journal of Theoretical Biology* **86**, 629–648.

VAN DRIESSCHE, W. & GULLENTOPS. K. (1982). Conductance fluctuation analysis in epithelia, *Techniques in Cellular Physiology* **P123**, 1–13.

VAN DRIESSCHE, W. & HILLYARD, S. D. (1985). Quinidine blockage of K$^+$ channels in the basolateral membrane of larval bullfrog skin. *Pflügers Archiv* **405**, suppl. 1, S77–82.

VAN DRIESSCHE, W., HILLYARD, S. D. & CANTIELLO, H. (1985). Investigations of basolateral K$^+$ channels of the tadpole skin epithelium with noise analysis. *Federation Proceedings* **44**, 1567.

VAN DRIESSCHE, W. & LINDEMANN, B. (1978). Low-noise amplification of voltage and current fluctuations arising in epithelia. *Review of Scientific Instruments* **49**, 52–57.

VAN DRIESSCHE, W., WILLS, N. K., HILLYARD, S. D. & ZEISKE, W. (1982). K$^+$ channels in an epithelial 'single membrane' preparation. *Archives internationales de physiologie et de biochimie* **90**, P12–14.

VAN DRIESSCHE, W. & ZEISKE, W. (1980). Ba^{2+}-induced conductance of spontaneously fluctuating K$^+$ channels in the apical membrane of frog skin (*Rana temporaria*). *Journal of Membrane Biology* **56**, 31–42.

WILLS, N. K. (1981). Antibiotics as tools for studying the electrical properties of tight epithelia. *Federation Proceedings* **40**, 2202–2205.

WILLS, N. K., EATON, D. C., LEWIS, S. A. & IFSHIN, M. S. (1979). Current–voltage relationship of the basolateral membrane of a tight epithelium. *Biochimica et biophysica acta* **555**, 519–523.

WILLS, N. K., LEWIS, S. A. & EATON, D. C. (1979). Active and passive properties of rabbit descending colon: a microelectrode and nystatin study. *Journal of Membrane Biology* **45**, 81–108.